Since January 2020 Elsevier has created a COVID-19 resource centre with free information in English and Mandarin on the novel coronavirus COVID-19. The COVID-19 resource centre is hosted on Elsevier Connect, the company's public news and information website.

Elsevier hereby grants permission to make all its COVID-19-related research that is available on the COVID-19 resource centre - including this research content - immediately available in PubMed Central and other publicly funded repositories, such as the WHO COVID database with rights for unrestricted research re-use and analyses in any form or by any means with acknowledgement of the original source. These permissions are granted for free by Elsevier for as long as the COVID-19 resource centre remains active.

CellPress

Cell Host & Microbe
Article

Bat Origins of MERS-CoV Supported by Bat Coronavirus HKU4 Usage of Human Receptor CD26

Qihui Wang,[1] Jianxun Qi,[1] Yuan Yuan,[1,2] Yifang Xuan,[3] Pengcheng Han,[4] Yuhua Wan,[1,5] Wei Ji,[6] Yan Li,[1] Ying Wu,[1] Jianwei Wang,[7] Aikichi Iwamoto,[8,9] Patrick C.Y. Woo,[10,11] Kwok-Yung Yuen,[10,11,12] Jinghua Yan,[1] Guangwen Lu,[1] and George F. Gao[1,2,3,6,12,13,*]

[1]CAS Key Laboratory of Pathogenic Microbiology and Immunology, Institute of Microbiology, Chinese Academy of Sciences, Beijing 100101, China
[2]School of Life Sciences, University of Science and Technology of China, Hefei 230027, Anhui Province, China
[3]Research Network of Immunity and Health, Beijing Institutes of Life Science, Chinese Academy of Sciences, Beijing 100101, China
[4]State Key Laboratory of Reproductive Biology, Institute of Zoology, Chinese Academy of Sciences, Beijing 100101, China
[5]School of Life Sciences, Anhui University, Hefei 230039, China
[6]National Institute for Viral Disease Control and Prevention, Chinese Center for Disease Control and Prevention (China CDC), Beijing 102206, China
[7]MOH Key Laboratory of Systems Biology of Pathogens, Institute of Pathogen Biology, Chinese Academy of Medical Sciences & Peking Union Medical College, Beijing 100730, China
[8]China-Japan Joint Laboratory of Molecular Microbiology and Molecular Immunology, Institute of Microbiology, Chinese Academy of Sciences, Beijing 100101, China
[9]Division of Infectious Diseases, Advanced Clinical Research Center, Department of Infectious Diseases and Applied Immunology, Research Hospital, University of Tokyo, Minato-ku, Tokyo 108-8639, Japan
[10]State Key Laboratory for Emerging Infectious Diseases, The University of Hong Kong, Pokfulam, Hong Kong Special Administrative Region 999077, China
[11]Department of Microbiology, The University of Hong Kong, Pokfulam, Hong Kong Special Administrative Region 999077, China
[12]Collaborative Innovation Center for Diagnosis and Treatment of Infectious Diseases, Zhejiang University, Hangzhou 310003, China
[13]Office of Director-General, Chinese Center for Disease Control and Prevention (China CDC), Beijing 102206, China
*Correspondence: gaof@im.ac.cn
http://dx.doi.org/10.1016/j.chom.2014.08.009

SUMMARY

The recently reported Middle East respiratory syndrome coronavirus (MERS-CoV) is phylogenetically closely related to the bat coronaviruses (BatCoVs) HKU4 and HKU5. However, the evolutionary pathway of MERS-CoV is still unclear. A receptor binding domain (RBD) in the MERS-CoV envelope-embedded spike protein specifically engages human CD26 (hCD26) to initiate viral entry. The high sequence identity in the viral spike protein prompted us to investigate if HKU4 and HKU5 can recognize hCD26 for cell entry. We found that HKU4-RBD, but not HKU5-RBD, binds to hCD26, and pseudotyped viruses embedding HKU4 spike can infect cells via hCD26 recognition. The structure of the HKU4-RBD/hCD26 complex revealed a hCD26-binding mode similar overall to that observed for MERS-RBD. HKU4-RBD, however, is less adapted to hCD26 than MERS-RBD, explaining its lower affinity for receptor binding. Our findings support a bat origin for MERS-CoV and indicate the need for surveillance of HKU4-related viruses in bats.

INTRODUCTION

Coronaviruses (CoVs) are a group of enveloped, single-stranded RNA viruses taxonomically affiliated with the *Coronaviridae* family (Lai et al., 2007). Based on genotypic and serological characteristics, coronaviruses are further classified into four species: *Alpha*, *Beta*, *Gamma* (King et al., 2012), and *Deltacoronavirus* (Woo et al., 2009). Both alpha (alphaCoVs) and betacoronaviruses (betaCoVs) can cause human diseases (Lai et al., 2007). Most human infections related to alpha and betaCoVs, such as coronaviruses NL63, 229E, OC43, and HKU1 (reviewed in Wevers and van der Hoek, 2009), which commonly manifest as self-limiting common cold-like illnesses, though more severe diseases can develop in children, the elderly, and immunocompromised patients (Chiu et al., 2005; Gorse et al., 2009; Jean et al., 2013; Jevšnik et al., 2012). BetaCoVs, however, can also be life threatening and have pandemic potential (Ksiazek et al., 2003; Zaki et al., 2012). In 2003, the severe acute respiratory syndrome coronavirus (SARS-CoV), a lineage B betaCoV (Lu and Liu, 2012), caused >8,000 infections and >800 deaths worldwide (WHO, 2004). In 2012, another lineage C betaCoV named the Middle East respiratory syndrome coronavirus (MERS-CoV) (King et al., 2012) initially emerged in Saudi Arabia (Bermingham et al., 2012; Zaki et al., 2012) and then spread to other countries in the Middle East, Europe, Asia, and the US, leading to 701 confirmed cases as of June 16th, 2014 (WHO, 2014) with a fatality rate of approximately 35%. These unexpected outbreaks highlight the public health significance of betaCoVs, especially those in lineages B and C.

In addition to MERS-CoV, lineage C betaCoVs include two other important members: the bat coronaviruses (BatCoVs) HKU4 and HKU5 (Lu and Liu, 2012). These viruses were first identified as genomes in 2006 in lesser bamboo bats

(*Tylonycteris pachypus*) and Japanese pipistrelles (*Pipistrellus abramus*), respectively (Woo et al., 2006), and remain circulating in bats (Lau et al., 2013). Bats have been implicated as the largest reservoir of alpha and betaCoVs (Li et al., 2005b; Woo et al., 2012) and play pivotal roles in interspecies transmission of coronaviruses. This is best exemplified by SARS-CoV, which was recently shown to originate from Chinese horseshoe bats (Ge et al., 2013) and likely transmitted directly to humans (Ge et al., 2013) or through an intermediate host such as the palm civet (Guan et al., 2003). The emergent MERS-CoV might also be of bat origin, with gene fragments being identified in bats from both Saudi Arabia (Memish et al., 2013) and Africa (Ithete et al., 2013) that are nearly identical to those of MERS-CoV in sequence. Despite the fact that the BatCoVs HKU4 and HKU5 are bat derived, the potential of both viruses evolving for human adaptation cannot be excluded because of their close phylogenetic relationship with MERS-CoV (Lau et al., 2013; Lu and Liu, 2012; van Boheemen et al., 2012). Nevertheless, such presumptions are largely based on their genomic features and phylogenetic status (Lau et al., 2013; Woo et al., 2006, 2007).

Virus infections initiate with the binding of viral particles to host surface cellular receptors. Identification of the functional receptors represents a central issue in studying viral pathogenesis. Several host peptidases, including aminopeptidase N (Delmas et al., 1992; Yeager et al., 1992) and angiotensin converting enzyme 2 (hACE2) (Hofmann et al., 2005; Li et al., 2003), are utilized by coronaviruses for cell entry. A timely study on MERS-CoV identified a third peptidase recognized by coronaviruses: dipeptidyl peptidase 4 (DPP4 or CD26) (Raj et al., 2013). This enzyme is a type II transmembrane protein contributing to the regulation of various physiological processes (Gorrell et al., 2001) and is "hijacked" by MERS-CoV to infect humans. This work pioneered the study on lineage C betaCoVs for potential cellular receptors. However, it remains unknown which molecules can be recognized by BatCoVs HKU4 and HKU5.

The receptor binding of coronaviruses is mediated by the spike (S) protein embedded in the viral envelope (Lai et al., 2007). In most cases, S is further cleaved by host proteases into S1 and S2 subunits that function to engage receptors and mediate membrane fusion, respectively (Lai et al., 2007). High sequence identities (>50%) in S have been observed between BatCoV HKU4/HKU5 and MERS-CoV (Lau et al., 2013), raising the possibility that these two viruses may use human CD26 (hCD26) as a receptor.

We previously delineated the molecular basis of MERS-CoV binding to hCD26. The S1 domain responsible for hCD26 recognition is located in a C-terminal 240-residue receptor binding domain (RBD) that is composed of a core and an external subdomain (Lu et al., 2013). The latter engages the receptor and is therefore also designated as the receptor binding motif (RBM) (Lu et al., 2013). Despite the overall high sequence identities in S, amino acid variance in the RBD region, especially in the RBM region, is still obvious among BatCoV HKU4, HKU5, and MERS-CoV. Investigation of the hCD26-binding potential of BatCoVs HKU4 and HKU5 is therefore a key to understanding the biology of these bat-derived viruses, their potential threat to human health, and the evolutionary pathway of MERS-CoV.

In this study, we demonstrated that the RBD domain of BatCoV HKU4 (HKU4-RBD), but not the equivalent domain of BatCoV HKU5 (HKU5-RBD), can bind to hCD26. The binding affinity between HKU4-RBD and hCD26 was determined by surface plasmon resonance (SPR) to be within the micromolar range. Despite the observed lower affinity compared to that between the MERS-CoV RBD (MERS-RBD) and hCD26, we found that pseudoviruses containing BatCoV HKU4 S can infect human Huh7 cells via hCD26. The findings provided solid evidence that BatCoV HKU4 recognizes hCD26 as a cellular receptor, indicating its potential for adaptation to infect humans. We further solved the complex structure of HKU4-RBD bound to hCD26 to delineate the basis of receptor recognition. Our structural analysis and mutagenesis also demonstrated a similar hCD26-binding mode between BatCoV HKU4 and MERS-CoV, but the details of variant amino acid interactions responsible for the differences in binding affinity are distinct. Our work also supports the notion that MERS-CoV most likely originated from bats.

RESULTS

HKU4-RBD, but Not HKU5-RBD, Binds to hCD26

Our previous study determined the hCD26-interacting region as an RBD spanning amino acids 367–606 of the MERS-CoV S (Lu et al., 2013). The phylogenetic relatedness between BatCoV HKU4/HKU5 and MERS-CoV (Figure 1A) prompted us to further investigate the equivalent RBD regions (S amino acids 372–611 for BatCoV HKU4, HKU4-RBD; and 375–604 for BatCoV HKU5, HKU5-RBD) in these bat-derived viruses for their potential to bind hCD26. A recent phylogenetic analysis of 13 BatCoV HKU4 and 15 BatCoV HKU5 strains revealed that the S gene of MERS-CoV is more closely related to BatCoV HKU4 than to BatCoV HKU5 (Lau et al., 2013). Using only the RBD amino acids, a concise phylogenetic tree was constructed, and a sequence alignment comparison was performed among BatCoV HKU4, HKU5, MERS-CoV, and SARS-CoV. Consistently, BatCoV HKU4 clustered with MERS-CoV with high bootstrap support, together joining BatCoV HKU5 to form an evolutionary branch distant from SARS-CoV (Figure 1A). At the sequence level, MERS-RBD exhibits identity to HKU4-RBD slightly higher than HKU5-RBD does (54.4% versus 52.9%). Nevertheless, the pairwise alignment clearly showed two marked deletions located in a region corresponding to the external subdomain of MERS-RBD in HKU5-RBD, but not in HKU4-RBD (Figure 1B). According to our previous study (Lu et al., 2013), this subdomain is responsible for receptor recognition. Therefore, we hypothesized that BatCoV HKU4 stands a better chance than BatCoV HKU5 of engaging hCD26.

Thus, we prepared the individual Fc fusion RBD proteins and tested their binding avidities to human hepatoma Huh7 cells (CD26-expressing) via flow cytometry. Consistent with previous reports (Raj et al., 2013), Huh7 cells express abundant hCD26 protein on their membrane surface (Figure 2A). MERS-RBD, as a natural viral ligand of hCD26, avidly binds to Huh7 cells. HKU4-RBD, but not HKU5-RBD, also bound to Huh7 cells (Figure 2B). Compared to MERS-RBD, however, an evidently smaller fluorescence shift was observed for HKU4-RBD, indicating a lower binding potency than MERS-RBD. An hCD26-specific antibody rather than an isocontrol immunoglobulin G (IgG) blocked the Huh7 surface attachment by HKU4-RBD (Figure 2C). The observed Huh7 binding was also inhibited by the soluble

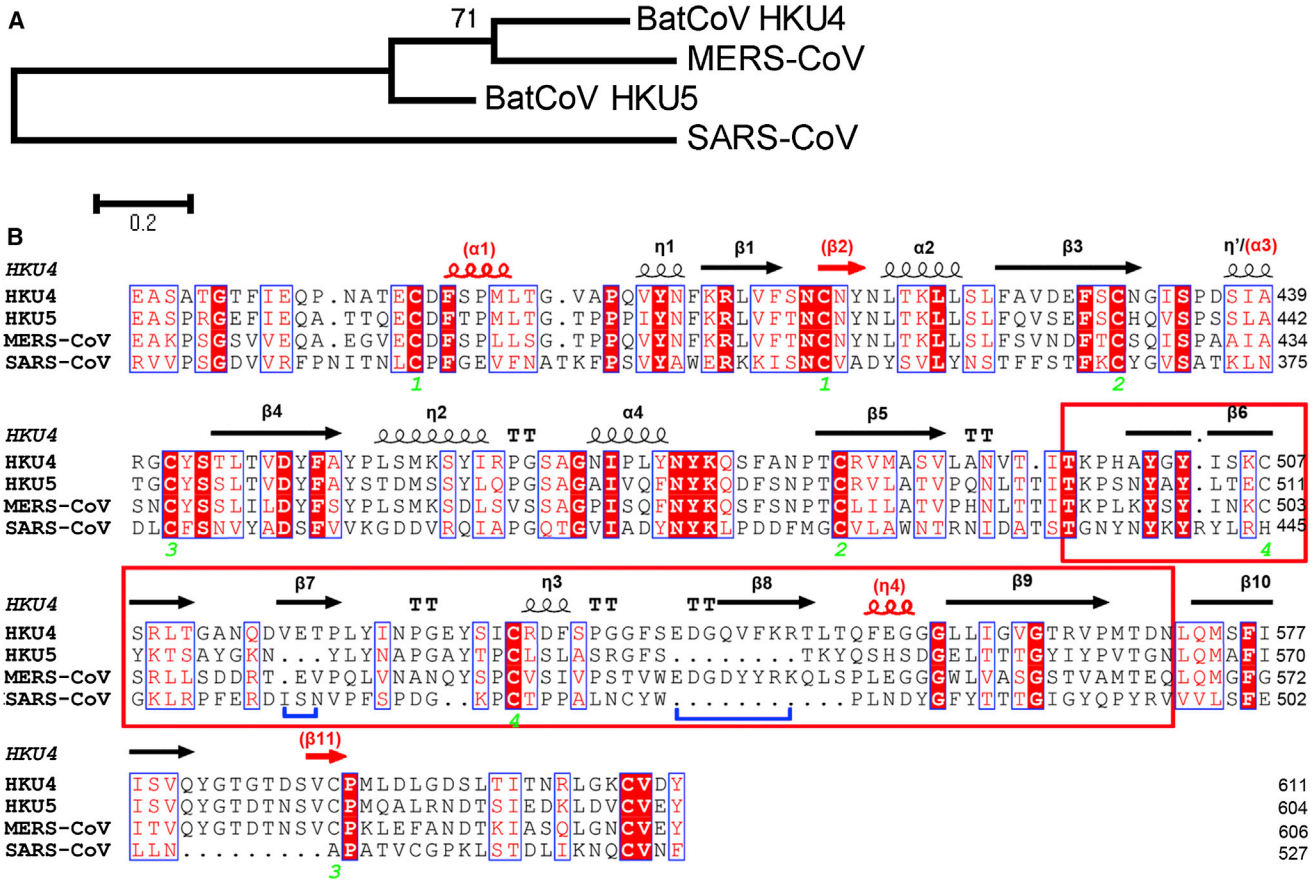

Figure 1. Comparison of the HKU4-RBD, HKU5-RBD, MERS-RBD, and SARS-RBD Sequences

(A) Phylogenetic tree generated using MEGA (Tamura et al., 2013) with the indicated RBD sequences.

(B) Structure-based sequence alignment. The secondary structure elements are defined based on an ESPript (Gouet et al., 1999) algorithm and are labeled as in a previous report on the MERS-RBD structure (Lu et al., 2013). Spiral lines indicate α or 3_{10} helices, while arrows represent β strands. Helices α1 and η4 and strands β2 and β11 are not preserved in the HKU4-RBD structure and are marked in red. The element equivalent to the MERS-RBD helix α3 exhibits characteristics of a 3_{10} helix in HKU4-RBD and is therefore labeled as η'. The external subdomain is highlighted by enclosure with a red box. The two deletions in HKU5-RBD are marked with blue lines. The Arabic numerals 1–4 indicate cysteine residues that pair to form disulfide bonds. See also Figure S3.

ectodomain protein of hCD26, but not by the extracellular fragment of the SARS-CoV receptor hACE2 (Figure 2D). We also utilized the hCD26-negative BHK cell line in the binding assay. As expected, surface binding to BHK cells could only be observed for HKU4-RBD and MERS-RBD after transfection of the cells with an hCD26-expressing plasmid (Figures 2E–2H). Taken together, these results clearly demonstrated that BatCoV HKU4, unlike its close relative BatCoV HKU5, is capable of binding to hCD26 via the spike-RBD region.

The Interaction between HKU4-RBD and hCD26 Is Specific but of Low Affinity

We next set out to characterize the interaction between HKU4-RBD and hCD26 using real-time biophysical binding assays. The proteins prepared from insect cells were purified to homogeneity (Figure S1, available online) and subjected to SPR experiments. As assay controls, MERS-RBD and SARS-RBD were found to bind potently to their respective canonical receptors (Figures 3A and 3B). HKU4-RBD interacted with hCD26, but not with hACE2 (Figures 3C and 3D). However, in contrast to the control pairs showing slow on and off rates, the Biacore binding profile between HKU4-RBD and hCD26 revealed fast association/dissociation kinetics. The equilibrium dissociation constant (K_D) of HKU4-RBD binding to hCD26 was calculated to be 35.7 μM (Figures 3C and S2), which is approximately three orders of magnitude lower than that of MERS-RBD to hCD26 (Lu et al., 2013). Though HKU5-RBD behaved similarly to its HKU4 homolog protein by gel filtration (Figure S1), no hCD26 binding was observed (Figure 3E), which is consistent with our flow cytometric assays (Figures 2B and 2F).

Cell Infection of BatCoV HKU4 Pseudoviruses Is Mediated by hCD26

With evidence of binding between HKU4-RBD and hCD26, we then tested the potential of this human surface molecule to function as a receptor for BatCoV HKU4. Lentiviral particles pseudotyped with either the BatCoV HKU4 or the MERS-CoV S were individually prepared in 293T cells. The successful incorporation of the viral S protein into the pseudovirus envelope was ascertained by western blotting using a monoclonal antibody

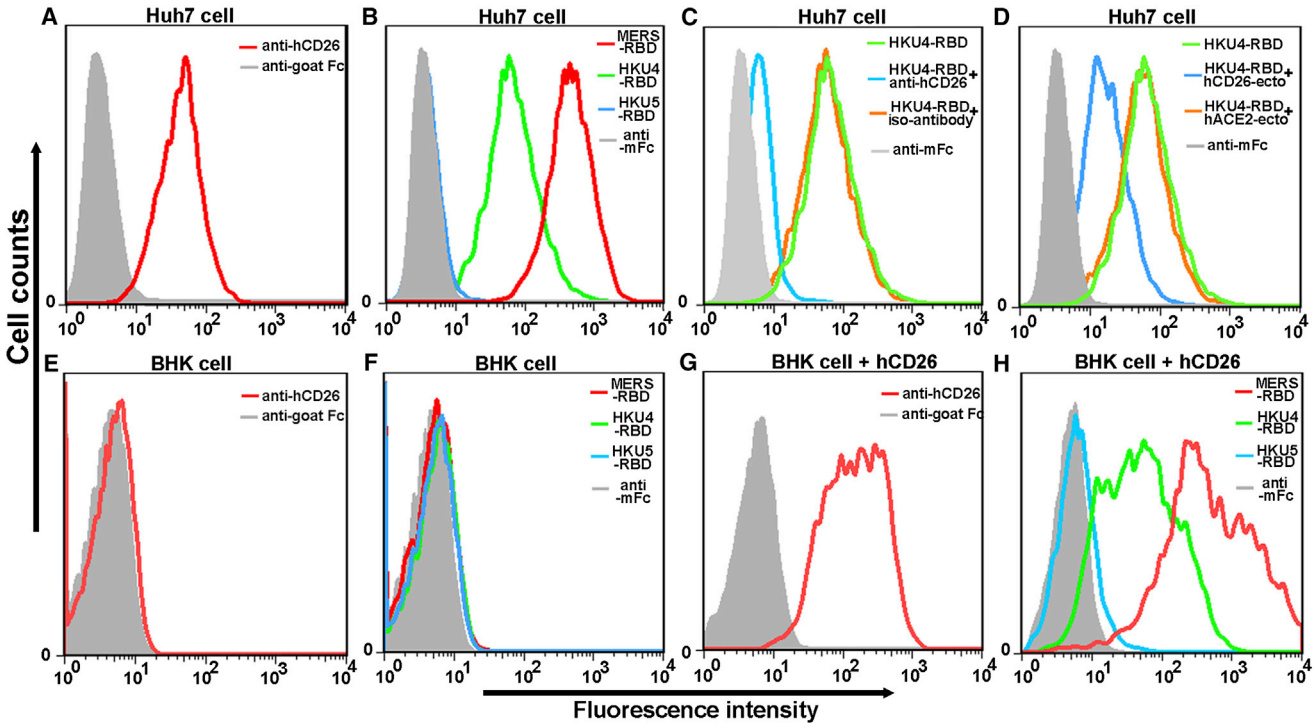

Figure 2. Characterization of Binding between HKU4-RBD and hCD26 by Flow Cytometry

(A) Huh7 cells stained with an anti-hCD26 antibody.

(B) Huh7 cells stained with MERS-RBD, HKU4-EBD, or HKU5-RBD.

(C) Huh7 cells stained with HKU4-RBD in the presence of an anti-hCD26 antibody or an isocontrol antibody.

(D) Huh7 cells stained with HKU4-RBD in the presence of hCD26 (hCD26-ecto) or hACE2 (hACE2-ecto) ectodomain protein.

(E) BHK cells stained with an anti-hCD26 antibody.

(F) BHK cells stained with MERS-RBD, HKU4-RBD, or HKU5-RBD.

(G) hCD26-transfected BHK cells stained with an anti-hCD26 antibody.

(H) hCD26-transfected BHK cells stained with MERS-RBD, HKU4-RBD, or HKU5-RBD.

recognizing a FLAG epitope engineered at the S C terminus (Figure 4A). In accordance with a previous report (Gierer et al., 2013), the majority of the MERS-CoV S protein was proteolytically cleaved (Figure 4A). In marked contrast, however, BatCoV HKU4 S remained largely intact (Figure 4A), displaying a pattern similar to that of SARS-CoV (Moore et al., 2004; Simmons et al., 2004).

The viral infection mediated by BatCoV HKU4 S was then tested in Huh7 cells. With a pseudotyped vector encoding luciferase, the infection efficiency was determined by quantifying luciferase activities in the cell lysates. As a positive control, pseudoparticles bearing the MERS-CoV S protein robustly infected Huh7 cells, showing an ~400-fold increase in the luciferase signal as compared to particles bearing no S protein. However, no evident cell infection was observed for the BatCoV HKU4 pseudoviruses (Figure 4B).

According to previous studies on other coronaviruses (reviewed in Simmons et al., 2013), proteolytic separation of the S protein into functional S1 and S2 subunits by host cell proteases is a prerequisite to subsequent membrane fusion. Noting the inefficient S proteolysis in the BatCoV HKU4 pseudoviruses above, we hypothesized that in vitro treatment of the virus particles with proteases such as trypsin might activate the S protein, enabling viral entry into the cells upon receptor recognition. Therefore, the harvested BatCoV HKU4 pseudovirus particles were treated with various concentrations of trypsin (2.5–40 μg/ml), incubated with fetal bovine serum to inactivate the trypsin, and then used to infect Huh7 cells. Proteolysis of the S protein was observed in a concentration-dependent manner for the pseudoviruses (Figure 4A). Accordingly, significant increases (>150-fold) in the luciferase activity were recorded for pseudoviruses pretreated with 10, 20, and 40 μg/ml of trypsin, demonstrating successful entry into the cells (Figure 4B). Then, pseudoviruses digested with 10 μg/ml trypsin were used in the subsequent antibody blocking assays. As expected, a concentration-dependent inhibition of cell infection was observed using the hCD26 antibody that specifically blocked the Huh7 surface attachment of HKU4-RBD (Figure 4C). Therefore, we provided direct evidence that pseudoviruses bearing BatCoV HKU4 S infect human cells via hCD26 recognition.

Complex Structure between HKU4-RBD and hCD26

We further used cocrystallography to study the molecular basis of binding between HKU4-RBD and hCD26. The two purified proteins were mixed in vitro to allow the formation of heterocomplexes, and we managed to solve the structure at a resolution of 2.6 Å (Table S1). In the crystallographic asymmetric unit, HKU4-RBD and hCD26 were observed to form two 1:1 binding

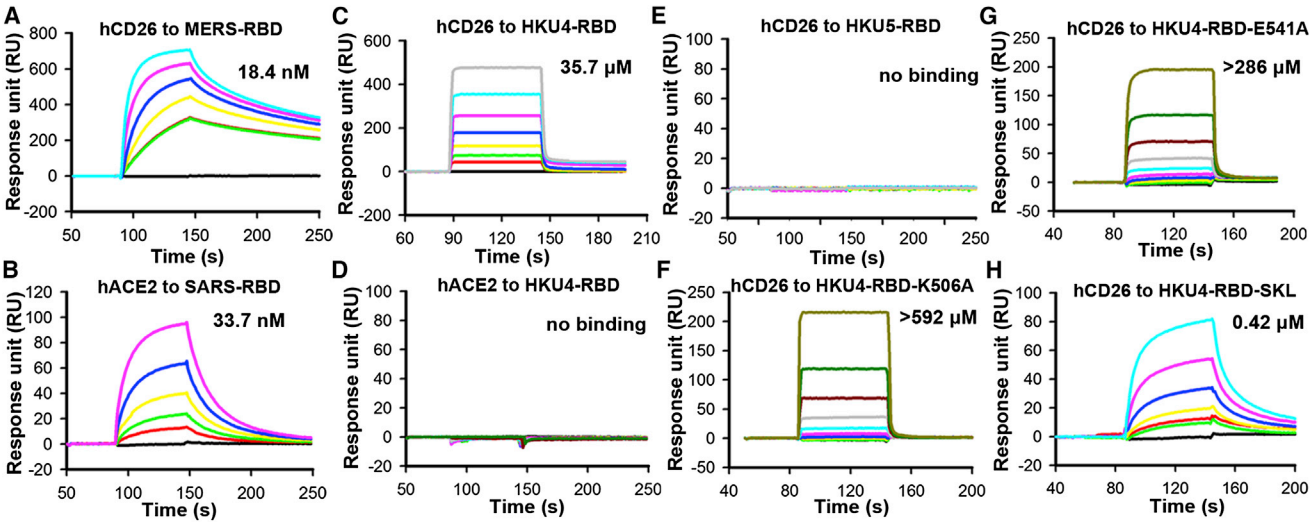

Figure 3. Specific Interaction between HKU4-RBD and hCD26 Characterized by SPR

(A–H) The indicated wild-type or mutant RBD proteins were immobilized on the chip and tested for binding with gradient concentrations of hCD26 or hACE2. The binding profiles are shown.

(A) hCD26 binding to MERS-RBD. (B) hACE2 binding to SARS-RBD. (C) hCD26 binding to HKU4-RBD. (D) hACE2 binding to HKU4-RBD. (E) hCD26 binding to HKU5-RBD. (F) hCD26 binding to HKU4-RBD-K506A. (G) hCD26 binding to HKU4-RBD-E541A. (H) hCD26 binding to HKU4-RBD-SKL, a triple mutant of S540W, K547R, and L558W. The dissociation constants were calculated to be 35.7 and 0.42 μM for the hCD26/HKU4-RBD and hCD26/HKU4-RBD-SKL pairs, respectively, and >400 μM for the hCD26/HKU4-RBD-K506A and hCD26/HKU4-RBD-E541A pairs. See also Figures S1 and S2.

complexes that are related by a two-fold axis (Figure 5A). These two complexes are of essentially the same structure, showing a root-mean-square deviation (rmsd) of ~0.18 Å for all Cα pairs. For hCD26, clear electron densities could be traced for 727 amino acids from R40 to P766. As observed in previous reports (Engel et al., 2003), this human enzyme folds into two structural domains: an α/β hydrolase domain and an eight-bladed β-propeller domain. hCD26 utilizes its propeller blades IV and V to recognize HKU4-RBD (Figures 5A and 5B). The two hCD26 molecules in the asymmetric unit were assembled into a dimer in the structure, with each protomer engaging one HKU4-RBD via its propeller. This leads to an overall U-shaped structure very similar to that observed for the MERS-RBD/hCD26 complex (Lu et al., 2013).

In the complex structure, HKU4-RBD contains 208 consecutive density-traceable residues, spanning T386 to L593. The folded structure comprises a core subdomain located distally from the engaging hCD26 and an external subdomain recognizing blades IV and V of the receptor propeller (Figure 5B). The core subdomain involves a five-stranded β sheet (β1, β3, β4, β5, and β10) forming a "nucleus" in the center, several helices (α helices α2 and α4, and 3_{10} helices η1, η′, and η2) decorating the center sheet on the exterior, and three disulfide bonds (C388/C412, C430/C483, and C442/C590) stabilizing the subdomain structure in the interior. The N and C termini are in close proximity, extending away from the bound receptor. The external subdomain is a strand-dominated structure with four anti-parallel β strands (β6–β9) and exposes a flat sheet-face for receptor engagement. An extra disulfide bond (C507/C531) located in this external region links helix η3 to strand β6 (Figures 1B and 5B).

As expected, this BatCoV HKU4 viral ligand exhibits significant structural homology to its MERS-CoV homolog, in agreement with the >50% sequence identity between the two molecules (Figure 1). Superimposition of the HKU4-RBD structure onto a previously reported MERS-RBD structure (Protein Data Bank [PDB]: 4KQZ) revealed an rmsd of ~1.1 Å for 194 equivalent Cα atoms. In comparison to MERS-RBD, the majority of the secondary structure elements are well preserved in HKU4-RBD. The latter, however, lacks an α helix (α1) and two small strands (β2 and β11) in its core subdomain and is devoid of a 3_{10} helix (η4) in the external subdomain. In addition, the helix preceding strand β3 exhibits characteristics of a 3_{10} helix (η′) in HKU4-RBD, rather than being α-helical (α3) as in MERS-RBD (Figures 1 and S3).

Atomic Details at the Binding Interface between HKU4-RBD and hCD26

In the complex structure, large surface areas (968.7 $Å^2$ in HKU4-RBD and 1,033.9 $Å^2$ in hCD26) are buried by the two binding entities. Therefore, we scrutinized this extended buried surface to identify key amino acids involved in complex formation. Residues located within the van der Waals (vdw) contact distance (4.5 Å resolution cutoff) between HKU4-RBD and hCD26 were selected (Table S2), and a series of hydrophilic amino acids located along the interface were found to form a solid network of H bond and salt bridge interactions (Figures 5B and 5C). These strong polar contacts include the HKU4-RBD residue K506 interacting with the receptor amino acids T288 and A289, N514 and Q515 with R317, D516 with Y322, E541 and D542 with K267, and K547 with I295 (Figure 5C). In addition, several residues (such as Y460 located in helix η2 of the RBD core subdomain) were further shown to contribute to the receptor binding by providing multiple vdw contacts (Table S2). It is notable that K506 and E541 of the viral ligand afforded both side-chain H bond and

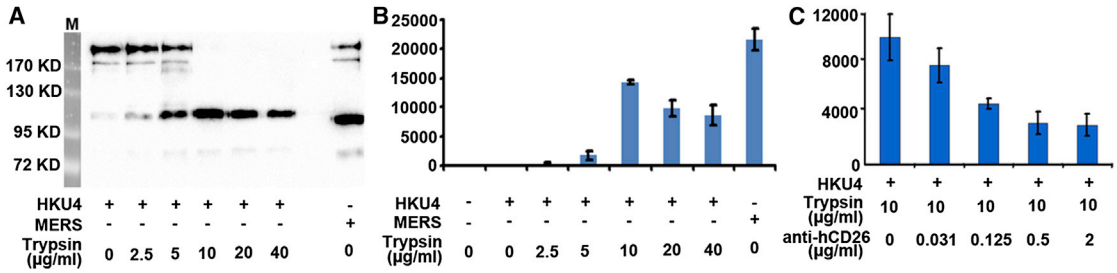

Figure 4. Huh7 Infection by Lentiviral Particles Pseudotyped with BatCoV HKU4 S

(A) Proteolytic processing of the embedded BatCoV HKU4 S by trypsin. The HKU4 pseudovirus was treated with trypsin at the indicated concentrations and characterized with an antibody recognizing a FLAG epitope engineered at the S C terminus. The untreated MERS pseudovirus was included as a reference control.

(B) A Huh7 cell infection assay with the indicated pseudoviruses.

(C) An antibody blocking assay using HKU4 pseudoviruses treated with 10 μg/ml trypsin and an anti-hCD26 antibody. The recorded fluorescence intensities were plotted as histograms, and the error bars represent ± SD for triplicate experiments.

multi-vdw interactions in this network (Table S2). Thus, these residues were individually mutated to alanine, and the resultant HKU4-RBD mutants were tested for receptor binding using SPR assays. The calculated K_Ds for the two mutants binding to hCD26 were >400 μM, which is an ~10-fold decrease in binding affinity compared to that of the wild-type protein (Figures 2F, 2G, and S2), demonstrating their important roles in receptor recognition. Interestingly, these two amino acids are conserved between HKU4-RBD and MERS-RBD (Figure 1B) and are also involved in the binding of the MERS-CoV ligand to hCD26 (Lu et al., 2013).

In addition to the aforementioned contact network, extra HKU4-RBD/hCD26 interactions involve a small hydrophobic patch (Figure 5D) and a sugar-mediated engagement (Figure 5E). The former is located in the proximity to a bulged hCD26 helix, which packs amino acids A291, L294, and I295 against RBD residues L510 and I560; the latter consists of a carbohydrate moiety linked to hCD26 N229 and amino acids E541 and Q544 in HKU4-RBD, which together form two H bonds.

Variant Amino Acid Interaction Details with hCD26 between HKU4-RBD and MERS-RBD

Overall, the HKU4-RBD/hCD26 structure solved in this study is very similar to the previously reported structure of MERS-RBD bound to hCD26. The two complex structures can be superimposed onto each other well, except for two interstrand loops (the β6/β7 and β8/β9 loops) in the RBD, which are distinctly oriented between the two viral ligands (Figure 6A). Despite variance in sequence, HKU4-RBD and MERS-RBD engage the same IV and V blades of the hCD26 β-propeller, demonstrating an overall similar recognition mode for hCD26 between BatCoV HKU4 and MERS-CoV.

We next compared the receptor binding details between the two viruses by characterizing the vdw contacts for each RBD residue along the binding interface. In both HKU4-RBD and MERS-RBD, a limited number of intermolecule contacts are contributed by the core subdomain residues, such as those located in the η2 (e.g., HKU4-Y460 and MERS-D455) and α4 (e.g., HKU4-N468 and MERS-P463) helices. These amino acids are adapted for hCD26 in HKU4-RBD slightly better than for that in MERS-RBD. For example, both HKU4-Y460 and HKU4-N468 provide more vdw contacts than the equivalent residues in MERS-RBD (Figures 6B and 6C).

In contrast to the core subdomain, with only limited contributions to hCD26 engagement, the majority of the ligand/receptor intermolecule contacts are provided by the amino acids located in the RBD external subdomain. Most HKU4 residues in this region contact hCD26 less efficiently than the corresponding MERS-RBD amino acids. Among these, the S540/W535 and K547/R542 pairs in the β8 strand and the L558/W553 pair in the β9 strand are most evident, each showing ~20–30 contact differences (Figures 6B and 6C). Reminiscent of the low binding affinity of HKU4-RBD to hCD26, these three residues in HKU4-RBD were mutated to the MERS-RBD amino acids, and the resultant mutant protein was tested for receptor binding by SPR. The calculated dissociation constant for this triple mutant was 0.42 μM, indicating that its binding affinity is ~100-fold greater than that of the wild-type parental protein. In addition, the mutation also shifted the binding kinetics from a fast-on/fast-off mode, as observed for the wild-type HKU4-RBD, to a slow-on/slow-off mode, as observed for the MERS-RBD (Figures 2H and S2). We believe that the resultant introduction of extra vdw contacts and hydrophobic interactions by substituting these three residues in HKU4-RBD with more hydrophobic amino acids (e.g., tryptophan) led to the change in the binding kinetics. A similar phenomenon of altered K_{on} and/or K_{off} rates resulting from changes in hydrophobic interaction has also previously been observed in other protein interactions (Weihofen et al., 2004).

DISCUSSION

Entry into susceptible host cells is the first step in the virus life cycle, and each entry process starts with receptor recognition. Identification of the cellular receptors for a virus is therefore a key question in viral pathogenesis studies. The BatCoVs HKU4 and HKU5 represent two important bat-derived coronaviruses closely related to MERS-CoV (Lau et al., 2013; van Boheemen et al., 2012). In this study, we performed a functional assay to identify potential receptors for these viruses. We found that HKU4-RBD, a protein domain spanning residues 372–611 of the BatCoV HKU4 S, but not the equivalent S region of BatCoV

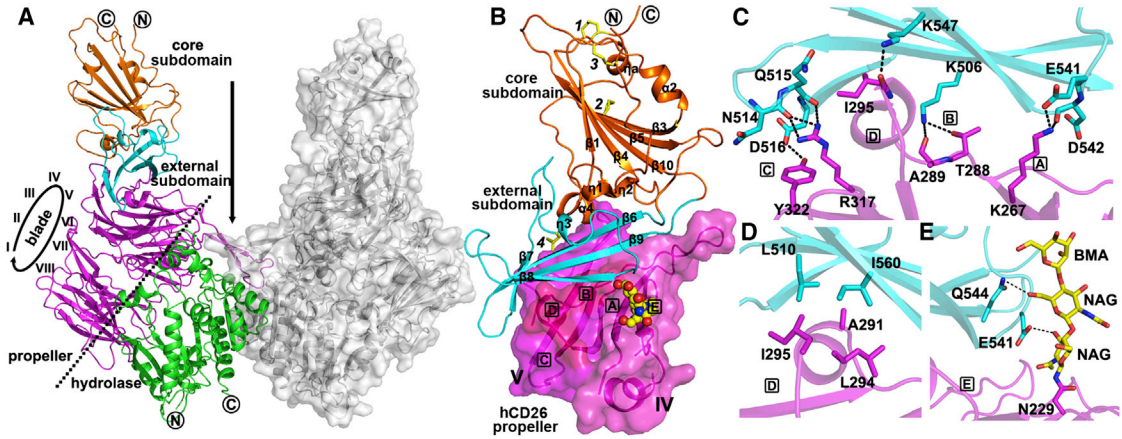

Figure 5. The Complex Structure of HKU4-RBD Bound to hCD26

(A) The overall structure. The two 1:1 complexes related by a two-fold axis (vertical arrow) are shown in cartoon and surface representations, respectively. The core and external subdomains of HKU4-RBD and the β-propeller and hydrolase domains of hCD26 are individually labeled and highlighted in orange, cyan, magenta, and green, respectively. The propeller blades (I–VIII) and the protein N/C termini are marked.

(B) A magnified view of the HKU4-RBD structure and the ligand/receptor interface. The secondary structure elements are specified by ESPript and labeled for the viral ligand. Yellow sticks marked with Arabic numbers indicate disulfide bonds. For the receptor, only propeller blades IV and V that engage HKU4-RBD are shown, using a surface representation.

(C–E) The important contact sites are marked with boxed letters A–E and are further delineated for interaction details as follows. (C) A solid network of H bond and salt bridge interactions. (D) A small patch of hydrophobic interactions. (E) Extra H bond contacts contributed by a carbohydrate moiety linked to hCD26 N229. The residues involved and the carbohydrates referred to are shown and labeled. See also Tables S1 and S2.

HKU5, binds to hCD26. In addition, the complex structure of HKU4-RBD bound to hCD26 was solved, demonstrating a receptor recognition mode similar to that observed for MERS-RBD, though with variant amino acid interaction details and a low binding affinity. We further showed that lentivirus particles pseudotyped with BatCoV HKU4 S could infect Huh7 cells via engagement of hCD26. Taken together, we provide the comprehensive data showing that hCD26 is also a functional receptor for the bat-derived HKU4 coronavirus. In support of this, a similar study of the functional reactivity of BatCoV HKU4 S for hCD26 was recently reported online (Yang et al., 2014) during the revision of our manuscript.

Coronavirus S proteins are among the typical class I membrane fusion proteins (Gao, 2007; Harrison, 2008; Xu et al., 2004a, 2004b). Activation of the subsequent membrane fusion process requires, in most cases, proteolysis of the fusion proteins by host cell proteases. This proteolytic process either occurs during or after maturation of the viruses, such as with murine hepatitis virus (MHV) (Frana et al., 1985) and MERS-CoV (Gierer et al., 2013), or occurs during viral entry, such as with SARS-CoV (Simmons et al., 2013). When we analyzed the lentivirus particles, the pseudotyped BatCoV HKU4 S was predominantly uncleaved. Accordingly, we initially were unable to observe any infection of Huh7 cells by the HKU4 pseudoviruses. However, by mimicking the maturation process of MERS-CoV, we showed that treatment of the pseudoviruses with trypsin enabled hCD26-mediated Huh7 infection. These results demonstrated that engagement of a receptor by, and proteolytic activation of, the envelope S protein remain two prerequisite factors for BatCoV HKU4 infection, as with other coronaviruses (Simmons et al., 2013). By identifying hCD26 as a functional receptor for BatCoV HKU4, the spatiotemporal processing of its S protein to allow subsequent membrane fusion remains an unresolved issue that should be further explored in the future.

Our results should also shed light on virus isolation. Since the first identification of the full-length HKU4 genome in bats in 2006 (Woo et al., 2006), culturing of the viruses has been unsuccessful. Further trials should consider cell lines expressing hCD26 but displaying variant proteases (e.g., cathepsin L, furin/furin-like proteases, HAT, and TMPRSS2) that are commonly involved in the processing of coronavirus spikes (Simmons et al., 2013). Alternatively, including small amounts of trypsin during viral culturing may facilitate the viral infection and thereby progeny virus production.

The previous SARS epidemic and the recent emergence of MERS-CoV in the Middle East serve as a constant reminder of the importance of identifying potential newly emerging coronaviruses in their natural animal reservoirs. Bats are natural reservoirs of many alphaCoVs and betaCoVs, which provide viral genes for the genesis of newly emerging coronaviruses with interspecies transmission potential. Phylogenetic dating suggests three suspected interspecies jumps of animal betaCoVs into humans, two of which (the SARS-CoV and MERS-CoV) are very likely of bat origin (Ge et al., 2013; Ithete et al., 2013; Li et al., 2005b; Memish et al., 2013) and were circulating in bats before they "jumped" to an intermediate host (e.g., civets for SARS-CoV and dromedary camels for MERS-CoV) and/or to humans (Ge et al., 2013; Guan et al., 2003; Haagmans et al., 2014; Reusken et al., 2013). A recent study demonstrates the circulation of BatCoV HKU4 in bats in the past years (Lau et al., 2013). With the data in this study, we found that BatCoV HKU4 has evolved to utilize hCD26 as a functional receptor and therefore gained one of the key factors sufficing for interspecies transmission and human infection. This highlights the necessity for a

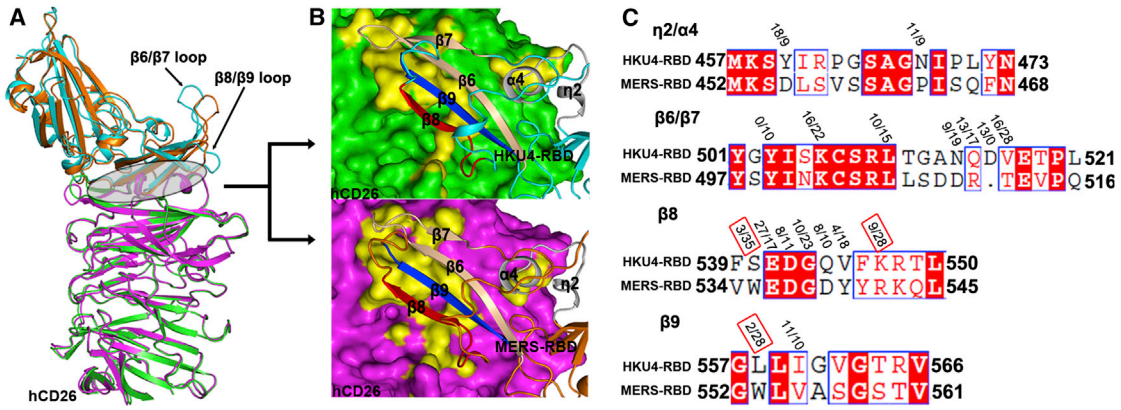

Figure 6. Comparison of the HKU4-RBD/hCD26 and MERS-RBD/hCD26 Pairs for Their Binding Modes and the Interaction Details

(A) Overall similar receptor binding mode between HKU4-RBD and MERS-RBD. Superimposition of the structure of HKU4-RBD (cyan) bound to hCD26 (green) and a complex structure of MERS-RBD (orange) with hCD26 (magenta). The loops exhibiting variant conformations are highlighted.

(B) A magnified view of the ligand/receptor (RBD in cartoon and hCD26 in surface) interface in the two binding pairs. The elements located within the vdw contact distance from the receptor are highlighted for the η2-α4 region (gray) in the core subdomain, and the β6-β7 (tint), β8 (red), and β9 (blue) strands in the external subdomain. Top: the HKU4-RBD/hCD26 structure. Bottom: the MERS-RBD/hCD26 structure.

(C) Better hCD26 adaptation in MERS-RBD than in HKU4-RBD. For each element specified in (B), the amino acid sequences were aligned between HKU4-RBD and MERS-RBD. The number pairs listed above the sequence highlight the differences in vdw contacts. For clarity, only those providing ≥10 intermolecule contacts are labeled. The S540/W535, K547/R542, and L558/W553 pairs showing the most contact differences are marked with red boxes.

surveillance program to monitor HKU4 circulation in bats. Special attention should be paid to virus variants incorporating mutations in S that would increase their affinity for hCD26 and/or confer susceptibility to host protease cleavage.

The complex structure presented in this study makes BatCoV HKU4 the sixth coronavirus in the *Coronaviridae* family for which the receptor-recognition mode has been elucidated with complex structures, in addition to SARS-CoV (Li et al., 2005a), MERS-CoV (Lu et al., 2013; Wang et al., 2013), MHV (Peng et al., 2011), NL63 (Wu et al., 2009), and porcine respiratory coronavirus (Reguera et al., 2012). Among these, BatCoV HKU4 likely represents a coronavirus suboptimized for receptor adaptation, displaying micromolar affinity for hCD26. Compared to MERS-CoV, which recognizes the same hCD26 molecule as a receptor (Raj et al., 2013), HKU4-RBD and MERS-RBD form similar structures and engage hCD26 via similar binding modes. Nevertheless, the two viral ligands exhibit a difference in receptor binding affinity of three orders of magnitude. We noted that in the RBM region predominating the ligand binding interface with the receptor, the majority of the interface residues in MERS-RBD contribute more vdw contacts than the equivalent amino acids in HKU4-RBD. This demonstrates a much better adaptation to hCD26 for MERS-CoV than for BatCoV HKU4, which was further supported by our mutagenesis data. We therefore presented the molecular basis for the observed affinity variance and a structural explanation for the suboptimized hCD26 binding by BatCoV HKU4. This weak binding also raises the possibility for the presence of other high-affinity receptors for BatCoV HKU4. Nevertheless, the physical interaction between HKU4-RBD and hCD26 seems to favor a scenario in which BatCoV HKU4 has evolved to adapt to the human receptor. In this sense, we cannot rule out the possibility that this bat-derived virus has been exposed, at some stage, to humans or human tissues.

Though with slight differences, the BatCoVs HKU4 and HKU5 exhibit similar sequence identities to MERS-CoV in the RBD region (54.4% versus 52.9%). The marked difference between the HKU4-RBD and HKU5-RBD relative to MERS-RBD, however, lies in two sequence deletions in the HKU5-RBD. Both deletions are located in the external subdomain and in two regions corresponding to the scaffold strands β7 and β8 in the MERS/HKU4-RBD structure. The deletions would therefore alter the fold of HKU5-RBM and abolish its interaction with hCD26. Similar amino acid deletions that exclude the viral ligand from interacting with hACE2 have also been recorded for diverse SARS-like coronaviruses identified in bats (Ren et al., 2008). An intact full-length external subdomain is likely a prerequisite to maintain binding capacity for hCD26 or hACE2, in addition to preserving key interacting residues, such as K506 and E541 in HKU4-RBD.

EXPERIMENTAL PROCEDURES

Gene Construction and Protein Expression

The coding sequences for target proteins were separately cloned into the EcoRI and *Xho*I restriction sites of pFastBac1 vector for baculovirus expression (Bac-to-Bac baculovirus expression system, Invitrogen). For each protein, an N-terminal gp67 signal peptide and a C-terminal hexa-His were added to facilitate protein secretion and purification. Sf9 cells were used to package and amplify the baculovirus, and High5 cells were used to express the proteins, which were purified by nickel affinity chromatography and gel filtration. The proteins were then used for crystallization and SPR experiments.

To prepare the Fc chimeric proteins, the fragments were fused 5′-terminally to a fragment coding for mouse Fc domain and ligated into the pCAGGS expression vector via the EcoRI and *Xho*I restriction sites. All fusion proteins were linked to the signal peptide of the MERS-CoV S protein. The proteins were transiently expressed in human embryonic kidney 293T (HEK293T) cells and purified by Protein A affinity chromatography and gel filtration. The purified proteins were then used for fluorescence-activated cell sorting (FACS) experiments (see Supplemental Experimental Procedures for detailed information).

Crystallization, Data Collection, and Structure Determination

For protein crystallization, monomeric HKU4-RBD was mixed with hCD26 at a 1:1 stoichiometry and crystallized by the sitting-drop vapor diffusion method at 4°C at 15 mg/ml in a buffer consisting of 0.1 M sodium citrate (pH 5.5) and 15%

PEG 6000. Diffraction data were collected with cryoprotected (in a reservoir solution containing 20% [v/v] glycerol) crystals at the Shanghai Synchrotron Radiation Facility (SSRF) BL17U. The complex structure was solved by molecular replacement using the structure of MERS-RBD/hCD26 (PDB: 4KR0) as the search model. For details, see Supplemental Experimental Procedures).

Binding Assays

Protein interactions were tested using both SPR analysis and FACS experiments. For the SPR assays, all proteins were exchanged into a buffer consisting of 10 mM HEPES (pH 7.4), 150 mM NaCl, and 0.005% v/v Tween 20. The indicated RBD proteins were immobilized onto CM5 chips and analyzed for real-time binding by flowing through gradient concentrations of hCD26 or hACE2.

For the cell sorting analysis, Huh7 or hCD26-transfected BHK cells were stained with different RBD-Fc fusion proteins and analyzed by flow cytometry. For the binding-block assay, Huh7 cells were incubated with an antibody (anti-hCD26 or anti-Flag; Sigma) or with the purified ectodomain protein (hCD26 or hACE2) before the addition of HKU4-RBD-mFc, then the cells were analyzed by cell sorting (for details, see Supplemental Experimental Procedures).

Pseudovirus Infection

BatCoV HKU4 pseudovirus particles were produced in HEK293T cells using a previously described method (Gao et al., 2013). For the pseudovirus infection, the virus particles were first treated with trypsin and then used to infect Huh7 cells in the presence or absence of the anti-hCD26 antibody. The luciferase activity was determined 48 hr postinfection using a GloMax 96 Microplate luminometer (Promega) (for details, see Supplemental Experimental Procedures).

ACCESSION NUMBERS

The atomic coordinate of the HKU4-RBD/hCD26 complex has been deposited in the Protein Data Bank with the PDB code 4QZV.

SUPPLEMENTAL INFORMATION

Supplemental Information includes Supplemental Experimental Procedures, three figures, and two tables and can be found with this article online at http://dx.doi.org/10.1016/j.chom.2014.08.009.

AUTHOR CONTRIBUTIONS

G.F.G. and G.L. initiated and coordinated the project. G.F.G., G.L., Q.W., and J.Y. designed the experiments. Q.W. conducted the experiments with help from Y.Y., Y.X., P.H., Y.W., W.J., and Y.L. J.Q. solved the structure. J.W. and A.I. provided the reagents and helped with manuscript writing. P.C.Y.W. and K.-Y.Y. helped with the data analysis and manuscript writing. Q.W., G.L., J.Y., and G.F.G. analyzed the data. G.L., Q.W., and G.F.G. wrote the manuscript.

ACKNOWLEDGMENTS

This work was supported by the National Natural Science Foundation of China (NSFC, Grant No. 81290342), the China National Grand S&T Special Project (No. 2014ZX10004-001-006), and the Strategic Priority Research Program of the Chinese Academy of Sciences (Grant No. XDB08020100). We thank the staff at the Shanghai Synchrotron Radiation Facility (SSRF) and Tong Zhao at the Institute of Microbiology, Chinese Academy of Sciences for support. G.F.G. is a leading principal investigator of the NSFC Innovative Research Group (Grant No. 81321063).

Received: May 14, 2014
Revised: July 30, 2014
Accepted: August 22, 2014
Published: September 10, 2014

REFERENCES

Bermingham, A., Chand, M.A., Brown, C.S., Aarons, E., Tong, C., Langrish, C., Hoschler, K., Brown, K., Galiano, M., Myers, R., et al. (2012). Severe respiratory illness caused by a novel coronavirus, in a patient transferred to the United Kingdom from the Middle East, September 2012. Euro Surveill. *17*, 20290.

Chiu, S.S., Chan, K.H., Chu, K.W., Kwan, S.W., Guan, Y., Poon, L.L., and Peiris, J.S. (2005). Human coronavirus NL63 infection and other coronavirus infections in children hospitalized with acute respiratory disease in Hong Kong, China. Clin. Infect. Dis. *40*, 1721–1729.

Delmas, B., Gelfi, J., L'Haridon, R., Vogel, L.K., Sjöström, H., Norén, O., and Laude, H. (1992). Aminopeptidase N is a major receptor for the entero-pathogenic coronavirus TGEV. Nature *357*, 417–420.

Engel, M., Hoffmann, T., Wagner, L., Wermann, M., Heiser, U., Kiefersauer, R., Huber, R., Bode, W., Demuth, H.U., and Brandstetter, H. (2003). The crystal structure of dipeptidyl peptidase IV (CD26) reveals its functional regulation and enzymatic mechanism. Proc. Natl. Acad. Sci. USA *100*, 5063–5068.

Frana, M.F., Behnke, J.N., Sturman, L.S., and Holmes, K.V. (1985). Proteolytic cleavage of the E2 glycoprotein of murine coronavirus: host-dependent differences in proteolytic cleavage and cell fusion. J. Virol. *56*, 912–920.

Gao, G.F. (2007). Peptide Inhibitors Targeting Virus-Cell Fusion in Class I Enveloped Viruses. In Combating the Threat of Pandemic Influenza: Drug Discovery Approaches, P.F. Torrence, ed. (New York: John Wiley & Sons), pp. 226–246.

Gao, J., Lu, G., Qi, J., Li, Y., Wu, Y., Deng, Y., Geng, H., Li, H., Wang, Q., Xiao, H., et al. (2013). Structure of the fusion core and inhibition of fusion by a heptad repeat peptide derived from the S protein of Middle East respiratory syndrome coronavirus. J. Virol. *87*, 13134–13140.

Ge, X.-Y., Li, J.-L., Yang, X.-L., Chmura, A.A., Zhu, G., Epstein, J.H., Mazet, J.K., Hu, B., Zhang, W., Peng, C., et al. (2013). Isolation and characterization of a bat SARS-like coronavirus that uses the ACE2 receptor. Nature *503*, 535–538.

Gierer, S., Bertram, S., Kaup, F., Wrensch, F., Heurich, A., Krämer-Kühl, A., Welsch, K., Winkler, M., Meyer, B., Drosten, C., et al. (2013). The spike protein of the emerging betacoronavirus EMC uses a novel coronavirus receptor for entry, can be activated by TMPRSS2, and is targeted by neutralizing antibodies. J. Virol. *87*, 5502–5511.

Gorrell, M.D., Gysbers, V., and McCaughan, G.W. (2001). CD26: a multifunctional integral membrane and secreted protein of activated lymphocytes. Scand. J. Immunol. *54*, 249–264.

Gorse, G.J., O'Connor, T.Z., Hall, S.L., Vitale, J.N., and Nichol, K.L. (2009). Human coronavirus and acute respiratory illness in older adults with chronic obstructive pulmonary disease. J. Infect. Dis. *199*, 847–857.

Gouet, P., Courcelle, E., Stuart, D.I., and Métoz, F. (1999). ESPript: analysis of multiple sequence alignments in PostScript. Bioinformatics *15*, 305–308.

Guan, Y., Zheng, B.J., He, Y.Q., Liu, X.L., Zhuang, Z.X., Cheung, C.L., Luo, S.W., Li, P.H., Zhang, L.J., Guan, Y.J., et al. (2003). Isolation and characterization of viruses related to the SARS coronavirus from animals in southern China. Science *302*, 276–278.

Haagmans, B.L., Al Dhahiry, S.H., Reusken, C.B., Raj, V.S., Galiano, M., Myers, R., Godeke, G.J., Jonges, M., Farag, E., Diab, A., et al. (2014). Middle East respiratory syndrome coronavirus in dromedary camels: an outbreak investigation. Lancet Infect. Dis. *14*, 140–145.

Harrison, S.C. (2008). Viral membrane fusion. Nat. Struct. Mol. Biol. *15*, 690–698.

Hofmann, H., Pyrc, K., van der Hoek, L., Geier, M., Berkhout, B., and Pöhlmann, S. (2005). Human coronavirus NL63 employs the severe acute respiratory syndrome coronavirus receptor for cellular entry. Proc. Natl. Acad. Sci. USA *102*, 7988–7993.

Ithete, N.L., Stoffberg, S., Corman, V.M., Cottontail, V.M., Richards, L.R., Schoeman, M.C., Drosten, C., Drexler, J.F., and Preiser, W. (2013). Close relative of human Middle East respiratory syndrome coronavirus in bat, South Africa. Emerg. Infect. Dis. *19*, 1697–1699.

Jean, A., Quach, C., Yung, A., and Semret, M. (2013). Severity and outcome associated with human coronavirus OC43 infections among children. Pediatr. Infect. Dis. J. *32*, 325–329.

Jevšnik, M., Uršič, T., Zigon, N., Lusa, L., Krivec, U., and Petrovec, M. (2012). Coronavirus infections in hospitalized pediatric patients with acute respiratory tract disease. BMC Infect. Dis. *12*, 365.

King, A.M.Q., Adams, M.J., Carstens, E.B., and Lefkowitz, E.J. (2012). Virus Taxonomy: Ninth Report of the International Committee on Taxonomy of Viruses. (London: Elsevier Academic Press).

Ksiazek, T.G., Erdman, D., Goldsmith, C.S., Zaki, S.R., Peret, T., Emery, S., Tong, S., Urbani, C., Comer, J.A., Lim, W., et al.; SARS Working Group (2003). A novel coronavirus associated with severe acute respiratory syndrome. N. Engl. J. Med. *348*, 1953–1966.

Lai, M.M.C., Perlman, S., and Anderson, L.J. (2007). Coronaviridae. In Fields Virology, D.M. Knipe and P.M. Howley, eds. (Philadelphia, PA: Lippincott Williams & Wilkins), pp. 1305–1335.

Lau, S.K., Li, K.S., Tsang, A.K., Lam, C.S., Ahmed, S., Chen, H., Chan, K.H., Woo, P.C., and Yuen, K.Y. (2013). Genetic characterization of Betacoronavirus lineage C viruses in bats reveals marked sequence divergence in the spike protein of pipistrellus bat coronavirus HKU5 in Japanese pipistrelle: implications for the origin of the novel Middle East respiratory syndrome coronavirus. J. Virol. *87*, 8638–8650.

Li, W., Moore, M.J., Vasilieva, N., Sui, J., Wong, S.K., Berne, M.A., Somasundaran, M., Sullivan, J.L., Luzuriaga, K., Greenough, T.C., et al. (2003). Angiotensin-converting enzyme 2 is a functional receptor for the SARS coronavirus. Nature *426*, 450–454.

Li, F., Li, W., Farzan, M., and Harrison, S.C. (2005a). Structure of SARS coronavirus spike receptor-binding domain complexed with receptor. Science *309*, 1864–1868.

Li, W., Shi, Z., Yu, M., Ren, W., Smith, C., Epstein, J.H., Wang, H., Crameri, G., Hu, Z., Zhang, H., et al. (2005b). Bats are natural reservoirs of SARS-like coronaviruses. Science *310*, 676–679.

Lu, G., and Liu, D. (2012). SARS-like virus in the Middle East: a truly bat-related coronavirus causing human diseases. Protein Cell *3*, 803–805.

Lu, G., Hu, Y., Wang, Q., Qi, J., Gao, F., Li, Y., Zhang, Y., Zhang, W., Yuan, Y., Bao, J., et al. (2013). Molecular basis of binding between novel human coronavirus MERS-CoV and its receptor CD26. Nature *500*, 227–231.

Memish, Z.A., Mishra, N., Olival, K.J., Fagbo, S.F., Kapoor, V., Epstein, J.H., Alhakeem, R., Durosinloun, A., Al Asmari, M., Islam, A., et al. (2013). Middle East respiratory syndrome coronavirus in bats, Saudi Arabia. Emerg. Infect. Dis. *19*, 1819–1823.

Moore, M.J., Dorfman, T., Li, W., Wong, S.K., Li, Y., Kuhn, J.H., Coderre, J., Vasilieva, N., Han, Z., Greenough, T.C., et al. (2004). Retroviruses pseudotyped with the severe acute respiratory syndrome coronavirus spike protein efficiently infect cells expressing angiotensin-converting enzyme 2. J. Virol. *78*, 10628–10635.

Peng, G., Sun, D., Rajashankar, K.R., Qian, Z., Holmes, K.V., and Li, F. (2011). Crystal structure of mouse coronavirus receptor-binding domain complexed with its murine receptor. Proc. Natl. Acad. Sci. USA *108*, 10696–10701.

Raj, V.S., Mou, H., Smits, S.L., Dekkers, D.H.W., Müller, M.A., Dijkman, R., Muth, D., Demmers, J.A.A., Zaki, A., Fouchier, R.A.M., et al. (2013). Dipeptidyl peptidase 4 is a functional receptor for the emerging human coronavirus-EMC. Nature *495*, 251–254.

Reguera, J., Santiago, C., Mudgal, G., Ordoño, D., Enjuanes, L., and Casasnovas, J.M. (2012). Structural bases of coronavirus attachment to host aminopeptidase N and its inhibition by neutralizing antibodies. PLoS Pathog. *8*, e1002859.

Ren, W., Qu, X., Li, W., Han, Z., Yu, M., Zhou, P., Zhang, S.Y., Wang, L.F., Deng, H., and Shi, Z. (2008). Difference in receptor usage between severe acute respiratory syndrome (SARS) coronavirus and SARS-like coronavirus of bat origin. J. Virol. *82*, 1899–1907.

Reusken, C.B., Haagmans, B.L., Müller, M.A., Gutierrez, C., Godeke, G.J., Meyer, B., Muth, D., Raj, V.S., Smits-De Vries, L., Corman, V.M., et al. (2013). Middle East respiratory syndrome coronavirus neutralising serum antibodies in dromedary camels: a comparative serological study. Lancet Infect. Dis. *13*, 859–866.

Simmons, G., Reeves, J.D., Rennekamp, A.J., Amberg, S.M., Piefer, A.J., and Bates, P. (2004). Characterization of severe acute respiratory syndrome-associated coronavirus (SARS-CoV) spike glycoprotein-mediated viral entry. Proc. Natl. Acad. Sci. USA *101*, 4240–4245.

Simmons, G., Zmora, P., Gierer, S., Heurich, A., and Pöhlmann, S. (2013). Proteolytic activation of the SARS-coronavirus spike protein: cutting enzymes at the cutting edge of antiviral research. Antiviral Res. *100*, 605–614.

Tamura, K., Stecher, G., Peterson, D., Filipski, A., and Kumar, S. (2013). MEGA6: Molecular Evolutionary Genetics Analysis version 6.0. Mol. Biol. Evol. *30*, 2725–2729.

van Boheemen, S., de Graaf, M., Lauber, C., Bestebroer, T.M., Raj, V.S., Zaki, A.M., Osterhaus, A.D., Haagmans, B.L., Gorbalenya, A.E., Snijder, E.J., and Fouchier, R.A. (2012). Genomic characterization of a newly discovered coronavirus associated with acute respiratory distress syndrome in humans. MBio *3*, e00473–e12.

Wang, N., Shi, X., Jiang, L., Zhang, S., Wang, D., Tong, P., Guo, D., Fu, L., Cui, Y., Liu, X., et al. (2013). Structure of MERS-CoV spike receptor-binding domain complexed with human receptor DPP4. Cell Res. *23*, 986–993.

Weihofen, W.A., Liu, J., Reutter, W., Saenger, W., and Fan, H. (2004). Crystal structure of CD26/dipeptidyl-peptidase IV in complex with adenosine deaminase reveals a highly amphiphilic interface. J. Biol. Chem. *279*, 43330–43335.

Wevers, B.A., and van der Hoek, L. (2009). Recently discovered human coronaviruses. Clin. Lab. Med. *29*, 715–724.

WHO (2004). Cumulative Number of Reported Probable Cases of Severe Acute Respiratory Syndrome (SARS). http://www.who.int/csr/sars/country/en/.

WHO (2014). Middle East respiratory syndrome coronavirus (MERS-CoV) – update. http://www.who.int/csr/don/2014_06_16_mers/en/.

Woo, P.C., Lau, S.K., Li, K.S., Poon, R.W., Wong, B.H., Tsoi, H.W., Yip, B.C., Huang, Y., Chan, K.H., and Yuen, K.Y. (2006). Molecular diversity of coronaviruses in bats. Virology *351*, 180–187.

Woo, P.C., Wang, M., Lau, S.K., Xu, H., Poon, R.W., Guo, R., Wong, B.H., Gao, K., Tsoi, H.W., Huang, Y., et al. (2007). Comparative analysis of twelve genomes of three novel group 2c and group 2d coronaviruses reveals unique group and subgroup features. J. Virol. *81*, 1574–1585.

Woo, P.C., Lau, S.K., Lam, C.S., Lai, K.K., Huang, Y., Lee, P., Luk, G.S., Dyrting, K.C., Chan, K.H., and Yuen, K.Y. (2009). Comparative analysis of complete genome sequences of three avian coronaviruses reveals a novel group 3c coronavirus. J. Virol. *83*, 908–917.

Woo, P.C., Lau, S.K., Lam, C.S., Lau, C.C., Tsang, A.K., Lau, J.H., Bai, R., Teng, J.L., Tsang, C.C., Wang, M., et al. (2012). Discovery of seven novel Mammalian and avian coronaviruses in the genus deltacoronavirus supports bat coronaviruses as the gene source of alphacoronavirus and betacoronavirus and avian coronaviruses as the gene source of gammacoronavirus and deltacoronavirus. J. Virol. *86*, 3995–4008.

Wu, K., Li, W., Peng, G., and Li, F. (2009). Crystal structure of NL63 respiratory coronavirus receptor-binding domain complexed with its human receptor. Proc. Natl. Acad. Sci. USA *106*, 19970–19974.

Xu, Y., Liu, Y., Lou, Z., Qin, L., Li, X., Bai, Z., Pang, H., Tien, P., Gao, G.F., and Rao, Z. (2004a). Structural basis for coronavirus-mediated membrane fusion. Crystal structure of mouse hepatitis virus spike protein fusion core. J. Biol. Chem. *279*, 30514–30522.

Xu, Y., Lou, Z., Liu, Y., Pang, H., Tien, P., Gao, G.F., and Rao, Z. (2004b). Crystal structure of severe acute respiratory syndrome coronavirus spike protein fusion core. J. Biol. Chem. *279*, 49414–49419.

Yang, Y., Du, L., Liu, C., Wang, L., Ma, C., Tang, J., Baric, R.S., Jiang, S., and Li, F. (2014). Receptor usage and cell entry of bat coronavirus HKU4 provide insight into bat-to-human transmission of MERS coronavirus. Proc. Natl. Acad. Sci. USA in press.

Yeager, C.L., Ashmun, R.A., Williams, R.K., Cardellichio, C.B., Shapiro, L.H., Look, A.T., and Holmes, K.V. (1992). Human aminopeptidase N is a receptor for human coronavirus 229E. Nature *357*, 420–422.

Zaki, A.M., van Boheemen, S., Bestebroer, T.M., Osterhaus, A.D., and Fouchier, R.A. (2012). Isolation of a novel coronavirus from a man with pneumonia in Saudi Arabia. N. Engl. J. Med. *367*, 1814–1820.